

## Power quality improvement and analysis of interconnected bus system with PMU using VSM-STATCOM

Preeti Kabra<sup>1</sup>, Donepudi Sudha Rani<sup>2</sup>

<sup>1</sup>Department of EEE, Deccan College of Engineering and Technology, Hyderabad, India

<sup>2</sup>Department of EEE, Sri Vasavi College of Engineering, Tadepalligudem, Andhra Pradesh, India

### Article Info

#### Article history:

Received Oct 19, 2021

Revised Jan 20, 2022

Accepted Jan 28, 2022

#### Keywords:

Graphical user interface

Non-conventional energy sources

Phasor measurement unit

Synchrophasors

Virtual synchronous machine–static synchronous compensator

### ABSTRACT

The traditional static synchronous compensator (STATCOM) present in the power grid to compensate instability problem will not be able to maintain stability of the system due to fluctuations in point of common coupling (PCC) voltage and frequency variation that may result in poor synchronization of the grid. The solution for this is the improvement in conventional STATCOM to virtual synchronous machine–static synchronous compensator (VSM-STATCOM). In this paper an interconnected IEEE-14 bus system is considered for analysis with VSM-STATCOM for improvement in voltage profile on weakest bus of the system. In order to find the weakest bus, load flow analysis is carried out on the bus system using Newton Raphson method. A VSM-STATCOM is connected at that weakest bus in synchronization to the grid injecting reactive power. For the analysis a fault is introduced on any of the line and voltage profile of the weakest bus is observed with and without VSM-STATCOM. The VSM-STATCOM is also compared to a conventional control STATCOM which has no inertia module. A comparative analysis is carried out with parameters of voltage magnitude and frequency of the weak bus taken into consideration. The voltage magnitude and frequency parameters of conventional STATCOM and VSM-STATCOM are measured using phasor measurement units. The model is designed using MATLAB Simulink power systems library block sets with graphical user interface (GUI) environment.

*This is an open access article under the [CC BY-SA](https://creativecommons.org/licenses/by-sa/4.0/) license.*



### Corresponding Author:

Preeti Kabra

Department of EEE, Deccan College of Engineering and Technology

Darussalam Rd, Darus Salam, Aghapura, Nampally, Hyderabad, Telangana 500001, India

Email: mail.preeti.kabra@gmail.com

## 1. INTRODUCTION

Most of the urban grid systems are designed and fabricated with interconnected bus system for sustainable power generation during failure of any source. The multiple sources availability at different bus locations helps the system to maintain power supply during failure [1] of any power generation unit. There is also an advantage of eliminating a complete line for repair from the grid during faults on the line, maintaining power [2] for the other lines with continuity of power supply. This elimination of faulty line from the grid system will mitigate damage to the equipment (sources and loads transmission lines) connected to it. As compared to radial distribution system the interconnected bus system has lower power quality problems. The major power quality issues [3]–[5] in any grid system are voltage sags and swells, harmonics in voltages and currents. Each power quality issue will be resolved with different devices, for harmonics problem active or passive filters are used whereas for voltage related problems and for reactive power

compensation flexible alternating current transmission system (FACTS) devices [6]–[10] like static var compensator (SVC), static synchronous compensator (STATCOM), dynamic voltage restorer (DVR), static synchronous series compensator (SSSC), and unified power quality conditioner (UPQC) are used. Each device has its own working principle compensating different parameters improving the voltage and current profiles and consequently power quality. A STATCOM [11] is introduced at the weakest bus of IEEE-14 bus [12] interconnected grid system for improvement of voltage profile. For finding the weakest bus in the grid system Newton Raphson method load flow analysis is used, which finds the lowest voltage magnitude bus from all the 14 buses. The single line diagram of the considered IEEE-14 bus system is as shown in Figure 1. This IEEE-14 bus system [13] has three generators (individual sources) and two synchronous compensators which inject reactive power. Each bus has its own load connected with different power rating.

The conventional STATCOM controller is later updated with virtual synchronous machine control included with virtual inertia updating the conventional STATCOM to virtual synchronous machine–static synchronous compensator (VSM-STATCOM). The effect of VSM-STATCOM to improve power quality of system with respect to conventional STATCOM is introduced here. The line parameters like line resistance and line reactance between different buses and generator rating data for the considered IEEE-14 bus system are shown in Table 1 and Table 2 respectively.

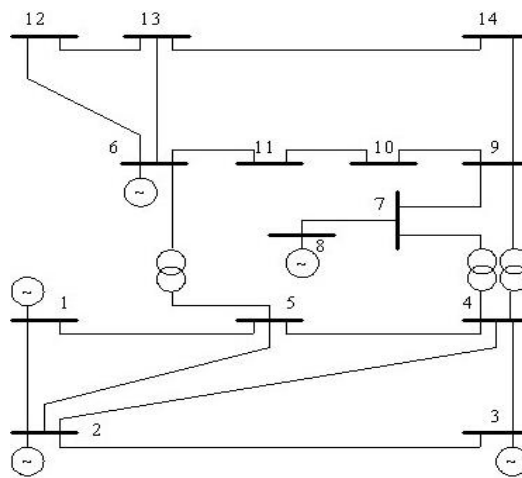


Figure 1. IEEE 14 bus system

Table 1. Bus system parameters

Line No.	From Bus	To Bus	Line Resistance ( $\Omega$ )	Line Reactance( $\Omega$ )
1	1	2	0.01948	0.05937
2	1	5	0.05503	0.23304
3	2	3	0.05799	0.19797
4	2	4	0.05322	0.17632
5	2	5	0.05495	0.17388
6	3	4	0.06301	0.17103
7	4	5	0.01435	0.04511
8	4	7	0	0.20712
9	4	9	0	0.56718
10	5	6	0	0.26802
11	6	11	0.09498	0.1989
12	6	12	0.13491	0.26881
13	6	13	0.07015	0.14227
14	7	8	0	0.16515
15	7	9	0	0.11521
16	9	10	0.03191	0.0925
17	9	14	0.14751	0.31048
18	10	11	0.09225	0.19287
19	12	13	0.23082	0.19728
20	13	14	0.18073	0.34242

Table 2. Generator rating data

Generator no.	P min (MW)	Pmax (MW)
1	10	160
2	20	80
3	20	50

**2. PHASOR MEASURING UNIT**

The Phasor measuring units also have global positioning system (GPS) installed along with parametric measuring, defining the position of the measurement. The phasor measurement units (PMUs) placed at different locations generally at the ends of the line or at different bus locations. The optimal placement of PMU [14] is decided by different algorithms like genetic algorithm, particle swarm optimization (PSO), and artificial bee colony (ABC). Phasor measuring units [15] are the devices which measure the magnitude, frequency and phase of any voltage or current of a grid system synchronized with universal time coordinate (UTC). The measurements [16] taken from the location are sent to wide area measuring system (WAMS), where the signals are compared for determination of phase shift in the angle and also voltage drops. With better measuring unit's precise measurements [17] are taken which are helpful with exact compensation value calculations for improving the power quality. PMUs use phase locked loop (PLL), analog to digital converters, signal filters, and GPS modules for synchronization measurement to the grid. The PLL generates the angle at which the voltage or current is generated or transmitted. A general internal structure of PMU can be shown in Figure 2.

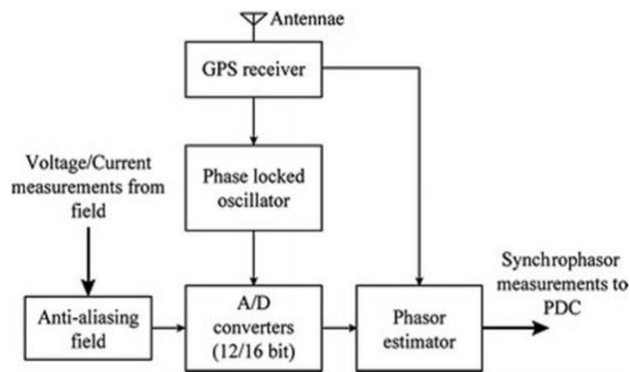


Figure 2. Architecture of PMU

The PMUs are connected in the proposed IEEE-14 bus system measuring the voltage magnitude, phases and frequencies of the grid system. As the modeling is in simulation GPS location is avoided in the measurement. Figures 3-6 represents voltage magnitude, frequency, current magnitude and phase angle at phase A of all the 14 buses with fault applied on the IEEE-14 bus system between 0.5 sec to 0.55 sec.

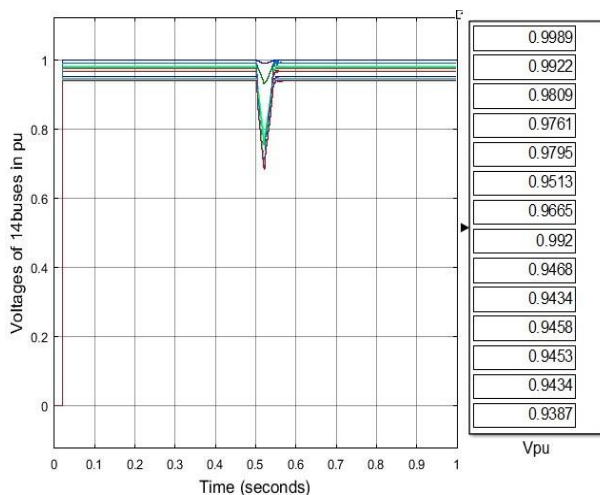


Figure 3. Voltage magnitudes of all buses

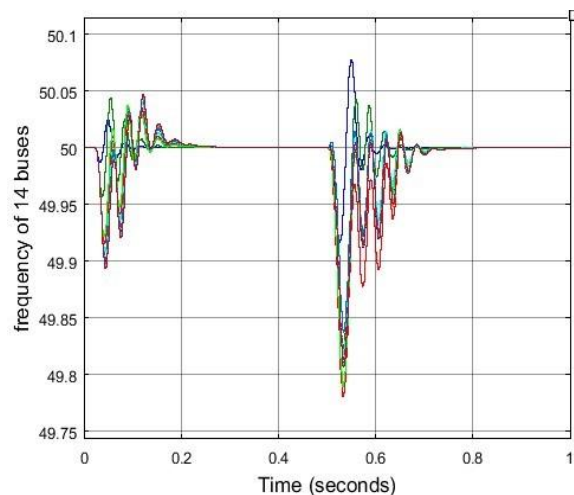


Figure 4. Frequencies of all buses

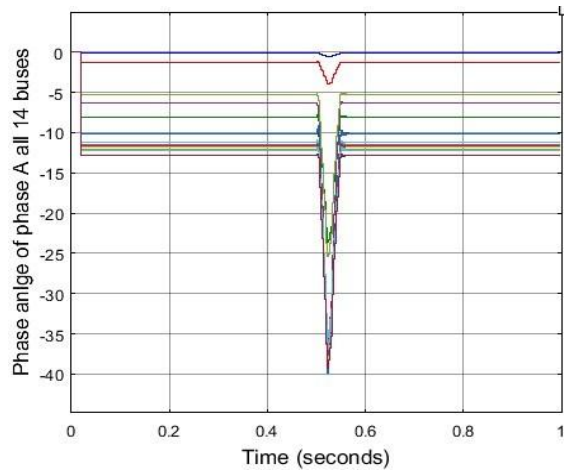


Figure 5. Current magnitudes of all buses

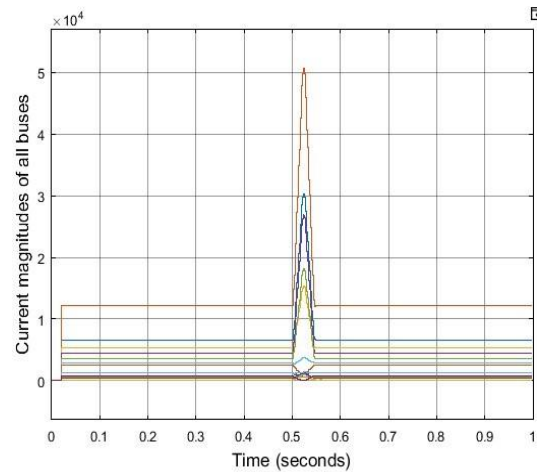


Figure 6. Phase angle at phase A of all buses

### 3. VSM-STATCOM MODELLING

The synchronization of VSM is done through Newton’s Law and swing equation which shows the movements of an imaginary rotating shaft as shown in Figure 7(a) which corresponds to 3 phase converters in Figure 7(b).

$$\frac{d\delta}{dt} = \omega - \omega_n \tag{1}$$

$$\frac{Mdw}{dt} - P_{dc} - P_{ac} - D(\omega - \omega_n)$$

where  $\delta$ -power angle,  $\omega$  and  $\omega_n$  are detected frequency and grid frequency respectively, M and D are virtual angular momentum and virtual damping coefficient,  $P_{dc}$  and  $P_{ac}$  are direct current ( $P_{ac}$ -DC) input active power and alternating current (AC) output active power of the converter. So, the imaginary shaft is rotating at the speed  $\omega$  which is driven by  $P_{dc}$  and braked by  $P_{ac}$ .

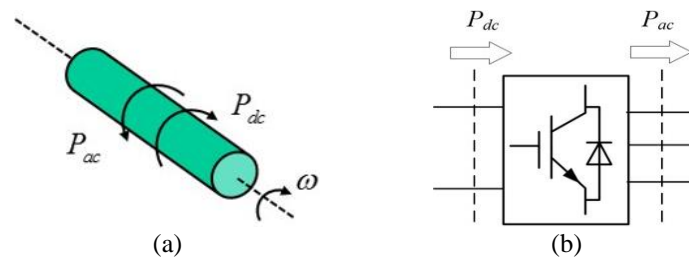


Figure 7. Virtual synchronous machine concept (a) imaginary rotating shaft and (b) 3-phase converter

The DC input power is a controllable variable and remains constant if commands are not given while with the power transfer equation the ac output power can be calculated.

$$P_{ac} = P_{max} \sin\delta \tag{2}$$

Where  $P_{max}$  is a constant relative to the operating condition. If  $\omega$  is greater than  $\omega_n$ ,  $\delta$  and  $P_{ac}$  will become larger, and then  $\omega$  will be decreased by the unbalance of input and output power, and vice versa. In the steady state, the two powers will be equal and the frequency will be eventually the grid frequency and hence the converter is synchronized with the grid. If (1) is implemented in the controller for the converter, the synchronization behavior will be exactly the same with the rotating shaft, showing an emulation of synchronous machines. A basic structure of VSM based controller is as shown in Figure 8. Control blocks of basic VSM controller with only virtual inertia presented where the transfer function  $G_{plant}$  represents the power transfe.

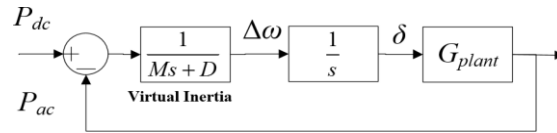


Figure 8. Control blocks of basic VSM controller

With increase in power demand and complexity of the grid system, it also needs to maintain the quality and stability of power supply [16]. In order to do that different power electronic devices [17] are connected to the grid in synchronization with the grid voltage. This is achieved by using PLL with synchronous reference frame (SRF) STATCOM control [18] devices which improve the power quality and stability. In this paper a STATCOM is introduced with VSM which mimics the conventional synchronous condenser.

The VSM device comprises as shown in Figure 9 of static power electronic switches controlled by PLL integrated controller with feedback from the grid voltage. For faster and robust controlling d-q components are used for generation of reference signals to generate pulse-width modulation (PWM) pulses for the power electronic devices connected in the VSM. The VSM parameters like virtual inertia and virtual impedance are implemented for the operation of STATCOM as a variable synchronous condenser device. A STATCOM device is considered for reactive power injection to improve power quality of the grid. The circuit topology of the device will however be the same only with the change in the controller. The proposed controller of the VSM-STATCOM [19], is given below, will be less sensitive to variation in voltage or power due to nonconventional energy sources or weak condition of grid and also providing better synchronization which results in better voltage regulation and ultimately improving power quality of the system.

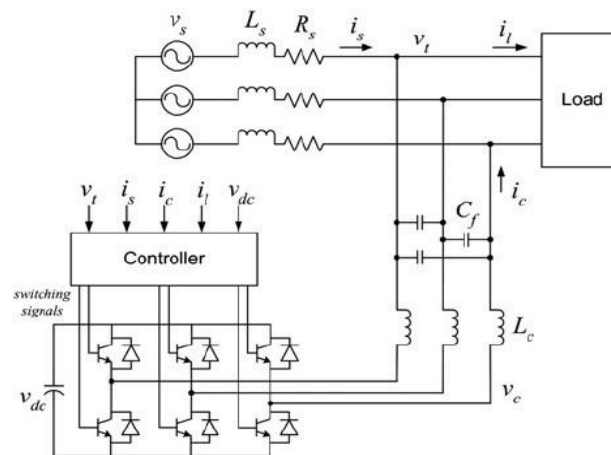


Figure 9. STATCOM circuit connected to grid for implementing the VSM

### 3.1. Conventional static synchronous compensator control

We need six pulses to make the voltage source converter (VSC) of the STATCOM to operate. The pulses to this converter are fed in synchronization to the grid with PCC voltage feedback. The controller of the conventional STATCOM [20] can be seen in Figure 10.

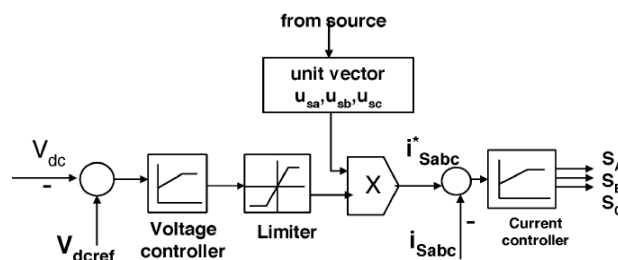


Figure 10. Conventional STATCOM control



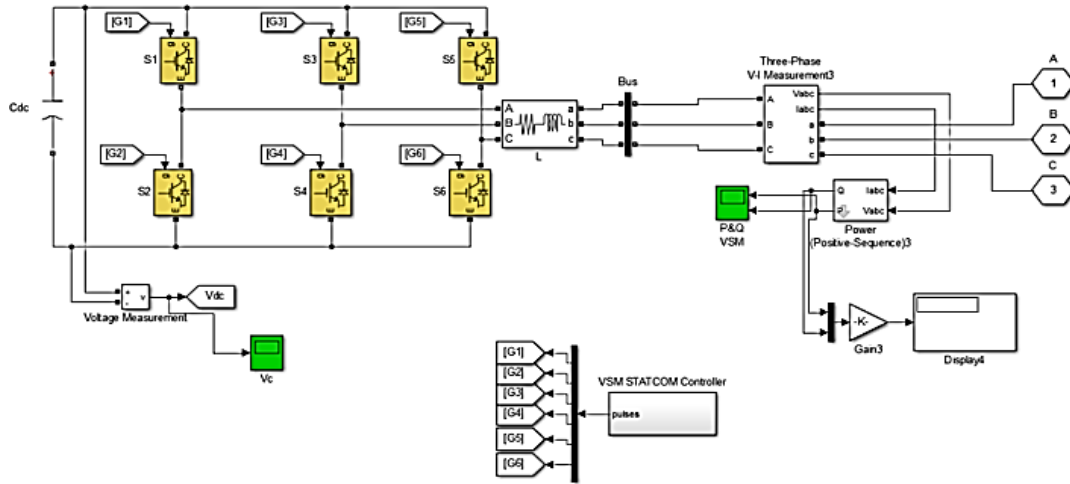


Figure 12. Control loops of VSM-STATCOM

**4.1. Design steps of virtual synchronous machine controller**

The design steps of virtual synchronous machine controller are: i) Finding the appropriate range for M and E with available dc capacitor size and DC voltage value; ii) Reduce the current compensators with appropriate value of the virtual inertia; iii) Selecting back EMF limit if it is needed; iv) Tuning the virtual inertia loop by changing D and M to get a desired bandwidth with required phase margin; v) Designing the R and L ratio for virtual impedance depending on the required harmonic spectrum; vi) Selecting the magnitude of the virtual impedance for enough damping for selected harmonic components; and vii) Designing compensators for the outer voltage loops. The virtual inertia of the STATCOM [26] is calculated using transfer function where D and M are virtual damping coefficient and virtual angular momentum given is Table 3. In similar way the virtual impedance is also calculated using transfer function with value of R and L given in Table 3.

Table 3. VSM-STATCOM parameters

Parameters	Value
Virtual angular momentum M	$5 \times 10^{-3} w_n$
Virtual damping factor D	$w_n$
Virtual resistance R	$0.1/\pi$
Virtual inductance L	50

Note:  $w_n$  - Fundamental Angular Frequency.

With the above value of virtual inertia and virtual impedance the controller is tuned with trial-and-error method for selecting the proportional integral (PI) gains [27] generating reference signals (d) for PWM generator. The change in angular frequency is given as:

$$\Delta w = (P_{dc} - P_{ac}) * \left( \frac{1}{M_S + D} \right)$$

From the fundamental and change in angular frequency the reference angle is generated as:

$$\theta = \int (w_n + \Delta w_n)$$

The reference voltage ‘e’ is generated by comparison of reference PCC voltage magnitude and measured PCC voltage magnitude given to PI controller. It is given as:

$$E^* = (K_p + \int K_i) * (|V_{pcc}^*| - |V_{pcc}|)$$

$$e = E^* \sin\theta$$

The reference voltage ‘e’ is compared to measured voltage of STATCOM ‘v’ and the error is fed to virtual impedance to generate reference current for the STATCOM. The final reference current is given as:

$$i^* = (e - v) \left( \frac{1}{Ls + R} \right)$$

The reference current ‘i\*’ dq components are compared to measured current ‘i’ dq components at the STATCOM output and the error is fed to PI controller [27]. With the above value of virtual inertia and virtual impedance the controller is tuned with trial-and-error method for selecting the PI gains generating reference signals (d) for PWM generator.

**5. LOAD FLOW ANALYSIS**

With the ‘powergui’ tool in the MATLAB Simulink software the load flow analysis is applied on the IEEE-14 bus system using Newton Raphson method and the weakest bus is identified from all the buses in the system. The load flow report generated by the analysis is as shown in Table 4, with the report generated it can be observed that voltage at bus 14 is recorded as the lowest value of 0.9446 pu and can be considered as weakest bus in the system. Therefore, the VSM-STATCOM is used for optimal placement of location at bus 14 to improve the voltage at the connected bus and also the buses near to the device and ultimately improving the power quality of the system. A comparative analysis is carried out on the system with voltage and frequency graphs generated with respect to time.

Table 4. Voltage and power result of load flow analysis of 14 buses

Bus ID	Vbase (kV)	V_LF (pu)	Vangle_LF (deg)	P_LF (MW)	Q_LF (Mvar)
BUS_1	11.00	1	0.00	40.13	7.62
BUS_2	11.00	1	0.00	21.70	12.70
BUS_2	11.00	1	0.00	208.66	41.18
BUS_3	11.00	0.9879	-6.90	0.00	-24.48
BUS_3	11.00	0.9879	-6.90	91.94	18.54
BUS_4	11.00	0.9825	-5.26	46.14	3.76
BUS_5	11.00	0.9854	-4.27	7.38	1.55
BUS_6	11.00	0.9573	-10.21	0.00	-11.67
BUS_6	11.00	0.9573	-10.21	10.26	6.87
BUS_7	11.00	0.9728	-9.09	0.00	0.00
BUS_8	11.00	0.9984	-9.17	0.00	-17.56
BUS_9	11.00	0.9529	-10.51	26.79	15.07
BUS_10	11.00	0.9494	-10.79	8.11	5.23
BUS_11	11.00	0.9518	-10.66	3.17	1.63
BUS_12	11.00	0.9512	-11.08	5.52	1.45
BUS_13	11.00	0.9494	-11.19	12.17	5.23
BUS_14	11.00	0.9446	-11.86	13.30	4.46

**6. RESULT ANALYSIS**

To observe the stability of the system, a fault is introduced at 0.5 for 2.5 cycles and removed at 0.55 sec. The fault introduced is three phase to ground balanced fault on IEEE-14 bus. The result observed with STATCOM, with and without VSM-STATCOM is as shown in Figure 13 for frequency and Figure 14 for voltage magnitude respectively. Table 4 shows the voltage magnitude, phase angle, active, and reactive power for all 14 buses after fault occurred. From the result it can be observed that voltage and frequency is controlled in better way compared to, with STATCOM and without VSM-STATCOM.

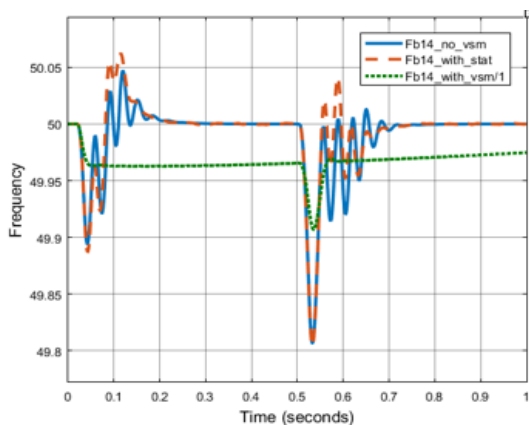


Figure 13. Frequency comparison of bus 14

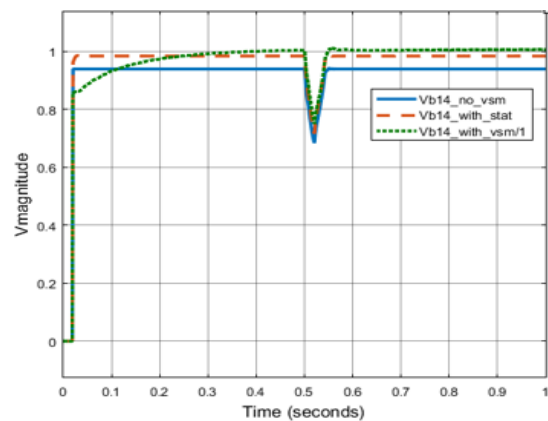


Figure 14. Voltage comparison of bus 14

## 7. CONCLUSION

The above result shows voltage magnitudes, frequencies, active and reactive power of all 14 buses, and the voltage profile of bus 14 is improved as it was identified as weakest bus using load flow analysis with Newton Raphson method. The voltage magnitude is increased to 1 pu gradually from 0.9446 pu condition and frequency of the bus is more stable as compared to without VSM-STATCOM and with conventional STATCOM. The disturbance and oscillations in the frequency are comparatively less with VSM-STATCOM after the fault is removed. So, we are finding the weakest bus and improving the power quality of power system in better way with VSM-STATCOM as compared to classical STATCOM and other conventional FACTS devices like UPQC or DVR as we are implementing the concept of virtual inertia and virtual impedance. So VSM-STATCOM is the better approach used to mitigate power quality issues during the integration of renewable energy sources.

## REFERENCES

- [1] A. A. P. Biscaro, R. A. F. Pereira, M. Kezunovic, and J. R. S. Mantovani, "Integrated Fault Location and Power-Quality Analysis in Electric Power Distribution Systems," *IEEE Transactions on Power Delivery*, vol. 31, no. 2, pp. 428–436, Apr. 2016, doi: 10.1109/TPWRD.2015.2464098.
- [2] F. Nejabatkhah, Y. W. Li, and H. Tian, "Power Quality Control of Smart Hybrid AC/DC Microgrids: An Overview," *IEEE Access*, vol. 7, pp. 52295–52318, 2019, doi: 10.1109/ACCESS.2019.2912376.
- [3] M. Moghbel, M. A. S. Masoum, A. Fereidouni, and S. Deilami, "Optimal Sizing, Siting and Operation of Custom Power Devices With STATCOM and APLC Functions for Real-Time Reactive Power and Network Voltage Quality Control of Smart Grid," *IEEE Transactions on Smart Grid*, vol. 9, no. 6, pp. 5564–5575, Nov. 2018, doi: 10.1109/TSG.2017.2690681.
- [4] S. Elphick, V. Gosbell, V. Smith, S. Perera, P. Ciufu, and G. Drury, "Methods for Harmonic Analysis and Reporting in Future Grid Applications," *IEEE Transactions on Power Delivery*, vol. 32, no. 2, pp. 989–995, Apr. 2017, doi: 10.1109/TPWRD.2016.2586963.
- [5] S. A. O. da Silva and F. A. Negrao, "Single-Phase to Three-Phase Unified Power Quality Conditioner Applied in Single-Wire Earth Return Electric Power Distribution Grids," *IEEE Transactions on Power Electronics*, vol. 33, no. 5, pp. 3950–3960, May 2018, doi: 10.1109/TPEL.2017.2723573.
- [6] M. M. Eladany, A. A. Eldesouky, and A. A. Sallam, "Power System Transient Stability: An Algorithm for Assessment and Enhancement Based on Catastrophe Theory and FACTS Devices," *IEEE Access*, vol. 6, pp. 26424–26437, 2018, doi: 10.1109/ACCESS.2018.2834906.
- [7] H. Nazari-pouya and S. Mehraeen, "Modeling and Nonlinear Optimal Control of Weak/Islanded Grids Using FACTS Device in a Game Theoretic Approach," *IEEE Transactions on Control Systems Technology*, vol. 24, no. 1, pp. 158–171, Jan. 2016, doi: 10.1109/TCST.2015.2421434.
- [8] A. H. Elmetwally, A. A. Eldesouky, and A. A. Sallam, "An Adaptive D-FACTS for Power Quality Enhancement in an Isolated Microgrid," *IEEE Access*, vol. 8, pp. 57923–57942, 2020, doi: 10.1109/ACCESS.2020.2981444.
- [9] Y. T. and X. Y. G. Yu, T. Lin, J. Zhang, "Coordination of PSS and FACTS damping controllers to improve small signal stability of large-scale power systems," *CSEE Journal of Power and Energy Systems*, vol. 5, no. 4, pp. 507–514, Aug. 2019, doi: 10.17775/CSEEJES.2018.00530.
- [10] J. Yu, Y. Xu, Y. Li, and Q. Liu, "An Inductive Hybrid UPQC for Power Quality Management in Premium-Power-Supply-Required Applications," *IEEE Access*, vol. 8, pp. 113342–113354, 2020, doi: 10.1109/ACCESS.2020.2999355.
- [11] N. A. Daw and A. H. Salih, "Choosing the Best Place of Static Var Compensator in IEEE 14 Bus System to Improve Voltage using Neplan Software," in *2019 19th International Conference on Sciences and Techniques of Automatic Control and Computer Engineering (STA)*, Mar. 2019, pp. 30–35, doi: 10.1109/STA.2019.8717247.
- [12] G. Bagha and A. Kumar, "Voltage Profile Enhancement for IEEE-14 Bus System using UPFC, TCSC and SSSC," in *2018 2nd IEEE International Conference on Power Electronics, Intelligent Control and Energy Systems (ICPEICES)*, Oct. 2018, pp. 267–272, doi: 10.1109/ICPEICES.2018.8897354.
- [13] S. K. Sah *et al.*, "Reactive Power Control of Modified IEEE 14 Bus System Using STATCOM," in *2018 Second International Conference on Intelligent Computing and Control Systems (ICICCS)*, Jun. 2018, pp. 335–339, doi: 10.1109/ICCONS.2018.8663177.
- [14] A. S. Siva, S. Sathieshkumar, and T. Santhosh Kumar, "Analysis of Stability in IEEE 14 Bus System using ETAP Software," in *2020 Fourth International Conference on Inventive Systems and Control (ICISC)*, Jan. 2020, pp. 935–938, doi: 10.1109/ICISC47916.2020.9171115.
- [15] Qing-Chang Zhong, Phi-Long Nguyen, Zhenyu Ma, and Wanxing Sheng, "Self-Synchronized Synchronverters: Inverters Without a Dedicated Synchronization Unit," *IEEE Transactions on Power Electronics*, vol. 29, no. 2, pp. 617–630, Feb. 2014, doi: 10.1109/TPEL.2013.2258684.
- [16] R. Rosso, S. Engelken, and M. Liserre, "Robust Stability Analysis of Synchronverters Operating in Parallel," *IEEE Transactions on Power Electronics*, vol. 34, no. 11, pp. 11309–11319, Nov. 2019, doi: 10.1109/TPEL.2019.2896707.
- [17] R. Rosso, J. Cassoli, G. Buticchi, S. Engelken, and M. Liserre, "Robust Stability Analysis of LCL Filter Based Synchronverter Under Different Grid Conditions," *IEEE Transactions on Power Electronics*, vol. 34, no. 6, pp. 5842–5853, Jun. 2019, doi: 10.1109/TPEL.2018.2867040.
- [18] L. Wang, C.-S. Lam, and M.-C. Wong, "A Hybrid-STATCOM With Wide Compensation Range and Low DC-Link Voltage," *IEEE Transactions on Industrial Electronics*, vol. 63, no. 6, pp. 3333–3343, Jun. 2016, doi: 10.1109/TIE.2016.2523922.
- [19] M. Morati, D. Girod, F. Terrien, V. Peron, P. Poure, and S. Saadate, "Industrial 100-MVA EAF Voltage Flicker Mitigation Using VSC-Based STATCOM With Improved Performance," *IEEE Transactions on Power Delivery*, vol. 31, no. 6, pp. 2494–2501, Dec. 2016, doi: 10.1109/TPWRD.2015.2508498.
- [20] C. Li, R. Burgos, B. Wen, Y. Tang, and D. Boroyevich, "Stability Analysis of Power Systems With Multiple STATCOMs in Close Proximity," *IEEE Transactions on Power Electronics*, vol. 35, no. 3, pp. 2268–2283, Mar. 2020, doi: 10.1109/TPEL.2019.2931891.
- [21] C. Li, R. Burgos, B. Wen, Y. Tang, and D. Boroyevich, "Analysis of STATCOM Small-Signal Impedance in the Synchronous d-q

- Frame,” *IEEE Journal of Emerging and Selected Topics in Power Electronics*, vol. 8, no. 2, pp. 1894–1910, Jun. 2020, doi: 10.1109/JESTPE.2019.2942332.
- [22] Y. Liu, X.-Y. Xiao, X.-P. Zhang, and Y. Wang, “Multi-Objective Optimal STATCOM Allocation for Voltage Sag Mitigation,” *IEEE Transactions on Power Delivery*, vol. 35, no. 3, pp. 1410–1422, Jun. 2020, doi: 10.1109/TPWRD.2019.2947715.
- [23] L. Huang, H. Xin, H. Yuan, G. Wang, and P. Ju, “Damping Effect of Virtual Synchronous Machines Provided by a Dynamical Virtual Impedance,” *IEEE Transactions on Energy Conversion*, vol. 36, no. 1, pp. 570–573, Mar. 2021, doi: 10.1109/TEC.2020.3040605.
- [24] M. Ebrahimi, S. A. Khajehoddin, and M. Karimi-Ghartemani, “An Improved Damping Method for Virtual Synchronous Machines,” *IEEE Transactions on Sustainable Energy*, vol. 10, no. 3, pp. 1491–1500, Jul. 2019, doi: 10.1109/TSTE.2019.2902033.
- [25] J. Roldan-Perez, A. Rodriguez-Cabero, and M. Prodanovic, “Design and Analysis of Virtual Synchronous Machines in Inductive and Resistive Weak Grids,” *IEEE Transactions on Energy Conversion*, vol. 34, no. 4, pp. 1818–1828, Dec. 2019, doi: 10.1109/TEC.2019.2930643.
- [26] A. Rodriguez-Cabero, J. Roldan-Perez, and M. Prodanovic, “Virtual Impedance Design Considerations for Virtual Synchronous Machines in Weak Grids,” *IEEE Journal of Emerging and Selected Topics in Power Electronics*, vol. 8, no. 2, pp. 1477–1489, Jun. 2020, doi: 10.1109/JESTPE.2019.2912071.
- [27] C. Li, R. Burgos, I. Cvetkovic, D. Boroyevich, L. Mili, and P. Rodriguez, “Analysis and design of virtual synchronous machine based STATCOM controller,” in *2014 IEEE 15th Workshop on Control and Modeling for Power Electronics (COMPEL)*, Jun. 2014, pp. 1–6, doi: 10.1109/COMPEL.2014.6877134.

## BIOGRAPHIES OF AUTHORS



**Preeti Kabra**    received B.E. degree in Electrical, Electronics and Power from Government college of Engineering, Aurangabad (MH) in 2000 and MTech degree from Jawaharlal Nehru Technical University, Hyderabad (TS). Currently working as Assistant Professor in Deccan College of Engineering and Technology, Hyderabad and Research scholar of KLEF, Vijaywada (AP). Her main area of interest is power system automation, smart grid, WAMS, and synchrophasor technology. She can be contacted at email: mail.preeti.kabra@gmail.com.



**Donepudi Sudha Rani**    received B. Tech degree in Electrical and Electronics Engineering from JNTU Hyderabad in 2006, M.E. degree from Andhra University in 2008, Visakhapatnam, and Doctoral degree from National Institute of Technology Warangal in 2016. Currently working as Professor in Sri Vasavi Engineering College, West Godavari, Andhra Pradesh. Her areas of interest are power system automation, smart grid, application of optimization in power systems, and electrical vehicles. She can be contacted at email: lakshmisudha124@gmail.com.